Performance evaluation of IEEE 802.15.4 with real time queueing analysis

Zhuoling Xiao [a],[*], Jie Zhou [a], Junjie Yan [b], Chen He [d], Lingge Jiang [d], Niki Trigoni [c]

[a] School of Communication and Information Engineering, University of Electronic Science and Technology of China, China
[b] School of Mathematical Sciences, University of Electronic Science and Technology of China, China
[c] Department of Computer Science, University of Oxford, OX1 1PD, UK
[d] Department of Electronic Engineering, Shanghai Jiao Tong University, Shanghai 200240, China

ARTICLE INFO

ABSTRACT

To provide a tool for performance evaluation of IEEE 802.15.4 with sleep mode enabled, a novel model based on real time queueing analysis is proposed in this paper. A low-rate wireless personal area network (LR-WPAN), composed of multiple nodes which send packets to the coordinator, is considered. The queueing behaviour of IEEE 802.15.4 node with sleep mode enabled differs from others because the packet arrivals in sleep period accumulate at the beginning of the active period, which makes a heavier load in the beginning than at any other time. This model analyses this behaviour by dividing the active portion of the superframe into backoff slots and then using an embedded discrete-time Markov chain model. The concept of virtual service time is introduced into this model which makes the proposed queueing model novel and different from typical ones. The accuracy of the proposed model is validated by Monte Carlo simulations in existing typical application scenarios, which indicates that the proposed queueing model can accurately evaluate the performance of IEEE 802.15.4 in the context of the application scenarios described in the simulations.

1. Introduction

ZigBee has gained significant attention in recent years, especially in ultra low power, low complexity and low data rate applications. Example applications range from building/home automation, remote control and smart energy management to home assisted health care. On the protocol design front, the MAC protocols that ZigBee relies on – IEEE 802.15.4 have gone through several major revisions [1,2] and amendments [3–5] since the first release in 2003. These revisions and amendments have significantly expanded the application of IEEE 802.15.4 in every aspect of our lives. However, the efficient use of ZigBee networks still hinges on the ability to predict and tune their performance in terms of key metrics, such as energy consumption and throughput. In this paper we advocate the need for analytical models for ZigBee networks, which are essential not only for performance estimation, but also for assisting in multiple facets of network operation, from protocol design to network topology setup and follow-on tuning.

However, accurate modelling of the protocol given arbitrary network conditions is extremely challenging for dynamic wireless networks. The most challenging problem is queueing analysis. It is the foundation of the whole network system and is closely correlated with all events in the network such as packet transmissions, collisions, and so on. The modelling of the protocol without taking the queueing behaviour into account makes the model inaccurate and less reliable in practice. In addition, due to the sleep mechanism introduced in the protocol for energy saving, the queue of each node in the network is time varying and thus cannot be simply modelled as a distribution. The real time queuing analysis instead of a simple distribution is essential for making the model sufficiently accurate for real time performance evaluation.

Although many models have been proposed for IEEE 802.15.4, none of these models provide a real time queueing analysis for performance evaluation, as discussed in Section 2. In this paper, a novel queueing model is proposed for IEEE 802.15.4 MAC with sleep mode enabled. We use an embedded discrete-time Markov chain to analyse the impact of real time load due to sleep mode on the performance of an IEEE 802.15.4 network. The proposed model consists of three submodels, including: (1) an embedded discrete-time Markov chain queueing model, which analyses the queueing

behaviour of IEEE 802.15.4 with sleep mode; (2) a virtual service time model, which provides an accurate virtual service time distribution using the backoff stage distribution; and (3) a CSMA/CA model, which studies the backoff mechanism of an IEEE 802.15.4 node and derives the backoff stage distribution.

The remainder of this paper is organized as follows. Section 2 provides an overview of related work. Section 3 presents the proposed queueing model and two related sub-models in detail, and derives important performance metrics. Section 4 compares numerical results from model derivation with simulation results and Section 5 concludes the paper.

2. Related works

In the literature, there are several works focused on the modelling and performance evaluations of IEEE 802.15.4 networks. The performance analysis by means of simulations and real experiments with IEEE 802.15.4 networks have been carried out in [6–8] and [9,10], respectively. But other studies, as described below, try to describe the behaviour of IEEE 802.15.4 networks with mathematical models which are used to evaluate the various performance metrics of this protocol.

A lot of good work has focused on analysing the CSMA/CA mechanism of IEEE 802.15.4 so far [11–14]. However, [11] and [12] use the same assumptions and formulations as the existing Bianchi's for IEEE 802.11 DCF [17] which is different from the mechanisms of IEEE 802.15.4. The accuracy of the model in [13] is not satisfactory because the authors simplify the analysis by approximating the uniform distribution for the random backoff counter in CSMA/CA process of IEEE 802.15.4 with a geometric distribution. Park et al. [14] proposed a novel way of approximating the probabilities of the two-slot sensing of CSMA/CA, where the success rate of the first CCA and second coupled with each other. However, this approximation did not take into account the difference of success rate at the beginning and end of a superframe due to different number of packets waiting to be sent.

Yoo et al. [15] have proposed a distance-constrained real-time message-scheduling algorithm to schedule a large number of real-time messages to meet their timing constraints. However, this paper does not present real-time analysis of the queuing behaviour and the derived performance of the whole network, as we do in this paper. Koubaa et al. [16] have analysed the performance of the guaranteed time slot (GTS) allocation mechanism in IEEE 802.15.4. The analysis gives a full understanding of the behaviour of the GTS mechanism with regards to delay and throughput metrics. GTS mechanism makes real-time guarantees possible for real-world applications. In comparison, the proposed model can analyse the FTS mechanism in a more comprehensive way.

Models in [18–23] have given accurate performance evaluations for the CSMA/CA mechanism of IEEE 802.15.4. Based on the previous work in [19], the model proposed in [21] analyses the slotted CSMA/CA of IEEE 802.15.4 in saturated condition, using embedded states to analyse the behaviour of nodes and the channel. Buratti has mentioned in [22] a similar modelling approach as ours by dividing the superframe into slots and analysing the behaviour of the node in each slot in order to evaluate the performance of both star-based and tree-based topologies in IEEE 802.15.4 LR-WPAN. [23] assumes that the number of pending packets waiting for transmission is no more than 1. All the above works model only the CSMA/CA process without queueing analysis and [18–21] even do not take the inactive period into account.

More recent research focuses on the performance modelling of IEEE 802.15.4 in specific applications [24–32]. For example, Karowski et al. [25] discuss the asynchronous multichannel discovery of IEEE 802.15.4. Zhu et al. [26] evaluate the performance of the protocol in large-scale wireless multi-hop sensor networks. Anbagi

et al. [27] propose the model for IEEE 802.15.4 in cyber physical power grid monitoring systems. Striccoli et al. [31] provide a model with a complete characterization of the frame-error-rate process. Govindan et al. [32] use Markov chain analysis for low data rate unsaturated traffic.

Only few work [33–35] take into consideration the queueing analysis and optional sleep mode. The queueing model based on an M/G/1/K system with vacations, proposed by Mišić et al., analyses the beacon enabled mode of an IEEE 802.15.4 cluster [33]. However, the assumption that every node enters sleep mode for a geometrically distributed time after its buffer becomes empty differs from the actual mechanism and makes the analytical results diverge from the simulation results. Another recent work [34] describes the queueing behaviour of IEEE 802.15.4 taking the optional sleep mode into account. But this work only considers single-slot channel sensing. Besides, it does not analyse the influence of inactive period on the queue length.

Our paper provides a novel analytical queueing model, taking the queueing details of an IEEE 802.15.4 node with sleep mode into account. Unlike models in [33] and [34], our study not only tell that the contention is intensive at the start of the superframe due to packet arrivals in the inactive period, but also provide quantitative results of the number of nodes competing for channel and the queue length of each node at any time of the superframe by dividing time into backoff slots and then using an embedded discrete-time Markov chain to model the queueing behaviour.

3. Analytical model formulation

3.1. IEEE 802.15.4

IEEE 802.15.4 is designed especially for ultra-low power networks consisting of battery-powered nodes. To address the energy consumption requirements, a simple and effective solution is to make nodes work in sleep/wakeup cycle. The sleep mode in IEEE 802.15.4, which enables nodes to enter a low-power mode periodically, is optional but crucial. Nodes do not listen to the channel in sleep mode. A detailed description of the benefits of sleep mode is provided in [36].

Two basic types of topology are supported by IEEE 802.15.4: star topology and peer-to-peer topology. The latter allows communications between two non-coordinator nodes, which makes it possible for a node to maintain multiple links with different nodes. The redundancy of links makes it possible for a node to deliver its packets to another node using different routes. On the other hand, the star topology is composed of several end nodes around a coordinator which serves as the center of the star topology. Each end node can only establish a single link and communicate with the coordinator, while communications between two end nodes are not supported. Compared with the peer-to-peer topology, the star topology is more effective in small area networks. Since it is widely accepted that IEEE 802.15.4 has difficulty in supporting large area networks, the star topology which is both simple and effective in small area networks is preferable in various applications such as wireless body area networks (WBAN) [37]. Moreover, it can be used as a construction unit to build other much more complicated network topologies such as the cluster tree topology. Therefore, in this research we consider a single-hop star topology with N identical end nodes and a coordinator.

Two types of channel access mode are supported in the MAC layer: the beacon and non-beacon mode. In the non-beacon mode, the unslotted CSMA/CA mechanism is used to wait for a random period and sense the channel before a packet is transmitted. The node can transmit the packet only when the channel is detected to be idle. Otherwise, it waits for another random period and senses the channel again. The key mechanisms of the beacon mode, in-
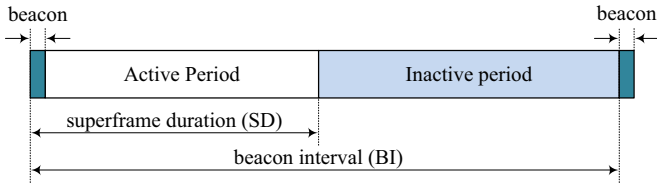
Fig. 1. Superframe structure of IEEE 802.15.4.

cluding superframe structure and slotted CSMA/CA, are both discussed together with the analytical model in Section 3.

As shown in Fig. 1, the superframe structure consists of an active period and an optional inactive period. The superframe is bounded by network beacons periodically transmitted by the PAN coordinator. The beacon interval *BI* and superframe duration *SD* are determined by the *macBeaconOrder* ($BO, 0 \leq BO \leq 14$) and *macSuperframeOrder* ($SO, 0 \leq SO \leq BO \leq 14$), respectively.

$$(BI, SD) = aBaseSuperframeDuration \times (2^{BO}, 2^{SO}) \qquad (1)$$

where *aBaseSuperframeDuration* is the minimum duration of a superframe, or numerically 15.32 ms.

Then, the duty cycle as a percent *D* which plays a pivotal role in the performance evaluation can be determined by the value of *BI* and *SD*, as

$$D = \frac{SD}{BI} \cdot 100 = 100 \cdot 2^{SO-BO}. \qquad (2)$$

3.2. Model assumptions

In this study, we consider the single-hop star topology with a PAN coordinator which serves as the center of the star network, and *N* nodes which can only communicate with the coordinator in active period using slotted CSMA/CA. All nodes with pending packets start the CSMA/CA algorithm in the active period of superframe to detect the channel in order to send the packet. Packets that cannot be transmitted in the current superframe will be transmitted in the next one.

The active period of the superframe is divided into backoff slots (denoted as slots hereafter) each of which has a duration of 20 symbols (or equivalently $T_B = 0.32ms$). The number of slots in the active and inactive period of superframe are denoted with T_A and T_I, respectively. Since O-QPSK modulation is used, with a bit rate of 250 kb/s, 10 bytes can be transmitted each slot. Therefore, the number of slots for a packet, denoted with T_P, may range from 1 to 13 because the maximal length of the packet is restricted to be no more than 133 bytes including the PHY and MAC headers in IEEE 802.15.4.

The hidden terminal problem is not taken into account; therefore, all nodes in the star network can hear each other. Similar assumptions are implemented in many studies [11,14,19–23]. Collisions may occur when two or more nodes detect a free channel and transmit the packet at the same time. No acknowledgment mechanism is implemented in this study for the sake of energy efficiency.

This model can accommodate a general traffic distribution on condition that the number of packets arriving in any two slots are independent of each other. We denote the arriving probability of *k* packets and no less than *k* packets during *t* slots with $q(k, t)$ and $Q(k, t)$, respectively.

Before we discuss the three sub-models in detail, we first give a whole picture of the three sub-models and their interactions, as shown in Fig. 2. In general, the embedded discrete-time Markov queueing model (or queueing model in short) uses both the virtual service time distribution ($p(\mathcal{T}_b, t)$) and the success probability of accessing the channel ($p_s(\mathcal{T}_b, t)$) from the virtual service time

model to determine the state transition matrix of Markov queuing model, which helps to generate the probability distribution of the number of competing nodes ($\mathcal{N}_c(t)$). The probability of number of competing nodes ($\mathcal{N}_c(t)$) is used in CSMA/CA model to determine the steady state probabilities of the CSMA/CA Markov chain which helps to calculate the distribution of backoff stages ($p_b(i, t)$). In the virtual service time model, the distribution of backoff stages ($p_b(i, t)$) is the key to both the virtual service time distribution and the success probability of accessing the channel.

3.3. Queueing model

To the best of our knowledge, the queueing behaviour of an IEEE 802.15.4 node is different from most existing typical queueing models due to the periodic sleeping. Since in practical applications the inactive period of the superframe is much longer than the active period, packets accumulate at the beginning of each superframe. With the subsequent transmissions, the buffer length gradually decreases and reaches its bottom at the end of the active period before it regains its maximum at the start of the next superframe. Therefore, the queue length here is time-varying and the periodic fluctuations in queue length affect the number of nodes that currently contend for the channel, which imposes significant influence on the service time of each packet.

To fully describe the dynamic queueing features of an IEEE 802.15.4 node, we implement the concept of virtual service time in our analysis. If some node in the network is transmitting, all other nodes with pending packets have to wait until the current transmission ends. If we define this wait as some kind of service, then every node is a virtual server for packets from all other nodes in the network (and a real server for its own packets of course). Then we define the wait time of a certain node for some packet in the network as the virtual service time. To make this concept clear, we tag a certain node in the network and study its behaviour in the rest of the paper.

The virtual service time $\mathcal{T}_v$ consists of three parts: $\mathcal{T}_b$ slots for backoff mechanism, 2 slots for clear channel assessment (CCA), and T_P slots for packet transmission. Let $p(\mathcal{T}_b, t)$ denote the probability that from the $(t + 1)$th slot of the superframe it takes $\mathcal{T}_b$ slots for some node in the network to firstly detect the channel and then start a new transmission. $p_s(\mathcal{T}_b, t)$ represents the probability that it is the tagged node that senses the channel in the $(t + \mathcal{T}_b + 1)$th slot provided it has packets waiting for transmission.

Let (n, t) stand for the state that the tagged node buffers *n* packets in the *t*th slot of the superframe where *n* takes value from 0 to L_m (the maximum queue length) and *t* ranges from 1 to T_A. Depending on whether the buffer of the node is empty and whether the remaining time in the current superframe is sufficient to complete the incoming backoff process and transmission, we have four distinct cases, namely, (1) empty buffer and sufficient time; (2) non-empty buffer and sufficient time for transmission; (3) non-empty buffer and sufficient time for backoff only; (4) non-empty buffer and insufficient time.

3.3.1. Empty buffer and sufficient time

The buffer of the node is empty in this situation. As a result, the node shall not contend for the channel and only transit to one of the states in the next slot of the superframe. Since no channel competition occurs, the state transition probabilities of this category are only determined by packet arrival probabilities $q(k, 1)$ and $Q(k, 1)$ (See Table 1 of notations). When $t = T_A$, the packet arrival duration is $T_I + 1$ and the next state is $(k, 1)$.

3.3.2. Non-empty buffer and sufficient time for transmission

From Fig. 3a which describes this situation, we can see that the tagged node has pending packets and meanwhile the remain-
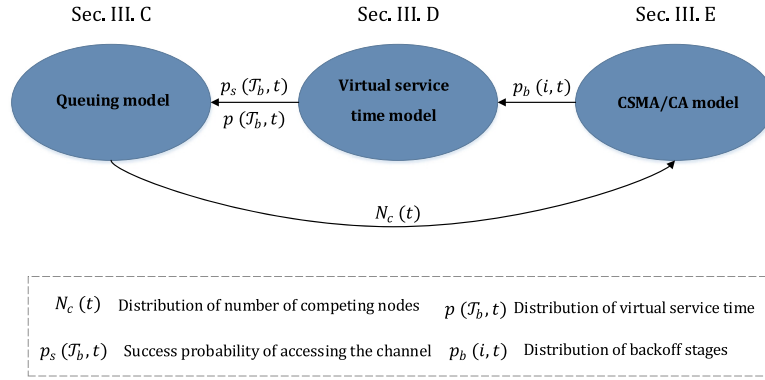
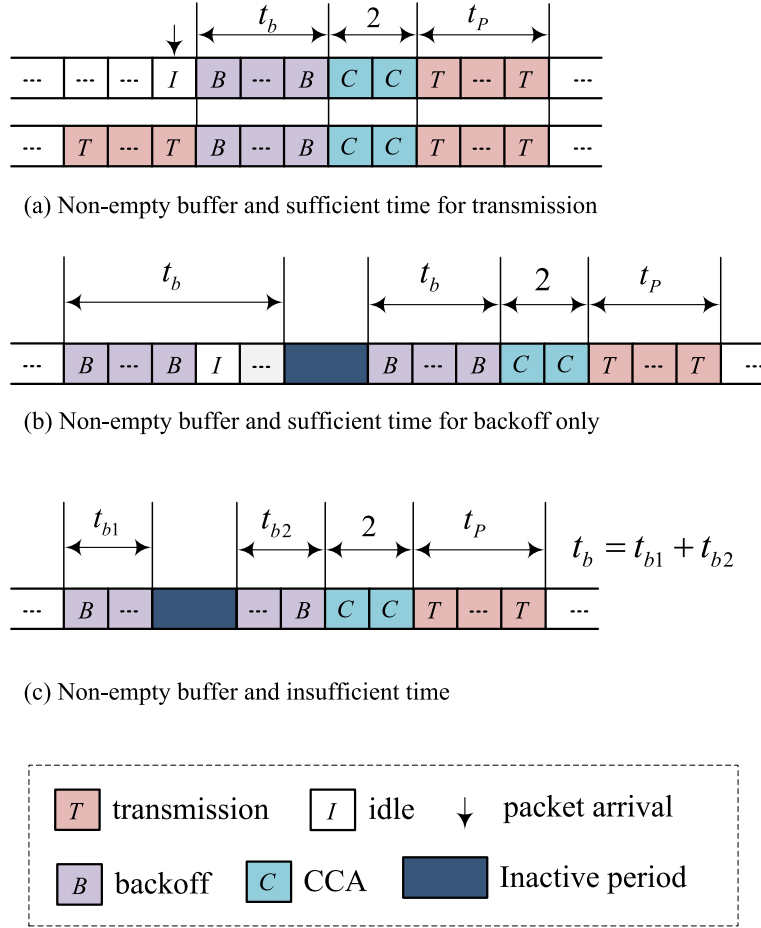Fig. 2. Sub-models and their interactions.

(a) Non-empty buffer and sufficient time for transmission

(b) Non-empty buffer and sufficient time for backoff only

(c) Non-empty buffer and insufficient time

Fig. 3. Slot timing for virtual service time.

ing time is sufficient for the incoming transmission, or mathematically $t + \mathcal{T}_v < T_A$. Therefore, the node shall transit from (n, t) to $(n + k, t + \mathcal{T}_v)(k = -1, 0, \ldots, L_m - n)$. However, in this situation, whether the node is idle in the tth slot makes a difference in the determination of virtual service time and should be treated separately. Details of the calculation of virtual service time are discussed in Section 3.4.

The state transition probabilities in this situation has two parts. If the tagged node succeeds in competing the channel, the transition probability is the product of the virtual service time distribution $p(\mathcal{T}_b, t)$, the conditional probability of the tagged node succeeds given the virtual service time period $p_s(\mathcal{T}_b, t)$, and the packet arrival probability $q(k + 1, \mathcal{T}_v)$. Similarly, if the tagged node

fails, the transition probability is $(1 - p_s(\mathcal{T}_b, t))p(\mathcal{T}_b, t)q(k, \mathcal{T}_v)$. Therefore, the transition probability from state (n, t) to $(n + k, t + \mathcal{T}_v)$ is given by

$$
\begin{aligned}
p((n + k, t + \mathcal{T}_v)|(n, t)) \\
= p_s(\mathcal{T}_b, t)p(\mathcal{T}_b, t)q(k + 1, \mathcal{T}_v) \\
+ (1 - p_s(\mathcal{T}_b, t))p(\mathcal{T}_b, t)q(k, \mathcal{T}_v).
\end{aligned} \tag{3}
$$

The above equation holds only when the buffer is not full, or $n + k < L_m$. Besides, when the buffer is full $(n + k \geq L_m)$, the transition probability is derived by replacing $q(k, t)$ with $Q(k, t)$.

Table 1
Notations used in this paper.

Notation	Description
D	The duty cycle
L_m	The buffer length
$\mathcal{T}_v$	The virtual service time
T_P	The transmission time
$\mathcal{T}_b$	The backoff time
T_B	The duration of a backoff slot
T_A	Number of slots in active period
T_I	Number of slots in inactive period
M	The maximum number of backoff stage
W_i	The length of the ith backoff stage
L_t	The queue length in the tth slot
S	Throughput (number of bits per second)
$\mathbb{E}(\mathcal{X})$	The expectation of random variable $\mathcal{X}$
$q(k, t)$	The probability of k packet arrivals within t slots
$Q(k, t)$	The probability of k packet arrivals at least within t slots
(n, t)	The Markov states defined in Queueing model
$\pi_{(n, t)}$	The steady state probability of state (n, t)
$p(\mathcal{T}_b, t)$	The probability of first channel sensing
$p_s(\mathcal{T}_b, t)$	The success channel access probability of the tagged node
$p_o(t)$	The idle probability of nodes in the t slot
$p_b(i, t)$	The probability of backoff stages
$p_d(\mathcal{T}_b, t)$	The probability that node performs CCA for the first time
$p_r(\mathcal{T}_b, t)$	The probability that node firstly senses the channel
$p_f(\mathcal{T}_b, t)$	The probability that node finds channel busy
$(s(t), w(t))$	The Markov states defined in CSMA/CA model
$\varphi_{(s(t), w(t))}$	The steady state probability of state $(s(t), w(t))$
$\mathcal{N}_c(t)$	The number of competing nodes in the tth slot
α	The probability that the channel is busy during the first CCA
β	The probability that the channel is busy during the second CCA
E	Energy consumption (mJ per bit)

$$p((L_m, t + \mathcal{T}_v)|(n, t))$$
$$= p_s(\mathcal{T}_b, t)p(\mathcal{T}_b, t)Q(L_m - n + 1, \mathcal{T}_v)$$
$$+ (1 - p_s(\mathcal{T}_b, t))p(\mathcal{T}_b, t)Q(L_m - n, \mathcal{T}_v) \qquad (4)$$

3.3.3. Non-empty buffer and sufficient time for backoff only

In IEEE 802.15.4, the MAC layer ensures that, after the random backoff, the remaining CSMA-CA operations can be undertaken and the entire transaction can be transmitted before the end of the active period. Therefore, if the remaining time in the active period is only sufficient to finish the concurrent backoff stage but insufficient to handle the subsequent steps, i.e., CCA and transmission, the MAC layer will start a new backoff process in the next superframe, which is illustrated in Fig. 3b.

This situation is equivalent to the situation that the tagged node delays $\mathcal{T}_b = T_A - t$ slots and then detects a busy channel ($p_s(\mathcal{T}_b, t) = 0$). According to the CSMA/CA process, it restarts the random delay process again in the $((t + \mathcal{T}_b) = T_A + 1)$th slot, which is the first slot of the next superframe. Therefore, nodes should transit from (n, t) to the first slot of the superframe $(n + k, 1)$, which means the time duration between the two states is $\tau = T_A + T_I - t$. Since in this case $p_s(\mathcal{T}_b, t) = 0$, referring to Eqs. (3) and (4), the transition probabilities can be determined as follows:

$$p((n + k, 1)|(n, t)) = p(\mathcal{T}_b, t)q(k, \tau), n + k < L_m, \qquad (5)$$

$$p((L_m, 1)|(n, t)) = p(\mathcal{T}_b, t)Q(L_m - n, \tau), n + k \geq L_m. \qquad (6)$$

3.3.4. Non-empty buffer and insufficient time

If the remaining number of slots in the active period is not sufficient to complete the backoff process, then the MAC layer freezes the backoff counter when it comes to the last slot in the active period and continues the counter from the first slot of the next superframe, as described in Fig. 3c. The transition probabilities in this situation are just the same as the ones discussed in Section 3.3.2 except for a greater buffer length caused by packet arrivals

in the inactive period. Taking the inactive period into account, the time duration of packet arrival in this situation is $\tau = \mathcal{T}_v + T_I$. Then similar to Eqs. (3) and (4) we have

$$p((n + k, \mathcal{T}_v - T_A + t)|(n, t))$$
$$= p_s(\mathcal{T}_b, t)p(\mathcal{T}_b, t)q(k + 1, \tau)$$
$$+ (1 - p_s(\mathcal{T}_b, t))p(\mathcal{T}_b, t)q(k, \tau), n + k < L_m, \qquad (7)$$

$$p((L_m, \mathcal{T}_v - T_A + t)|(n, t))$$
$$= p_s(\mathcal{T}_b, t)p(\mathcal{T}_b, t)Q(L_m - n + 1, \tau)$$
$$+ p_s(\mathcal{T}_b, t)p(\mathcal{T}_b, t)Q(L_m - n + 1, \tau). \qquad (8)$$

To determine $p(\mathcal{T}_b, t)$ and $p_s(\mathcal{T}_b, t)$ in the virtual service time model, we need the number of nodes competing for channel in the tth slot of the superframe given that the tagged node has pending packets, denoted by $\mathcal{N}_c(t)$. Assume in this study that each node in the network is independent of each other, the probability distribution of $\mathcal{N}_c(t)$ is

$$p(\mathcal{N}_c(t) = i) = \binom{N - 1}{i - 1}(1 - p_o(t))^{i-1}(p_o(t))^{N-i}, i = 1, 2, \ldots, N, \qquad (9)$$

where $p_o(t)$ is the idle probability of nodes in the tth slot, which is determined as $p_o(t) = T_A\pi_{(0,t)}$. In this paper, we denote the steady state probability of state (n, t) in the queueing model with $\pi_{(n, t)}$.

3.4. Virtual service time model

As stated, the virtual service time consists of three parts: the backoff time $\mathcal{T}_b$, the transmission time T_P, and the CCA time.

$$\mathcal{T}_v = \mathcal{T}_b + T_P + 2 \qquad (10)$$

Since T_P is a constant which can be easily determined by the data packet length and the transmission rate, the probability distribution of service time $p(\mathcal{T}_v, t)$ is only determined by the distribution of backoff time $p(\mathcal{T}_b, t)$. According to different states of the tagged node (in backoff state or not, at the start of the superframe or not), three situations are discussed and correspondingly different approximations are made.

3.4.1. Backoff state, not the start

In this situation we make the FIRST APPROXIMATION that if the tagged node is already in backoff state and some other node has been transmitting before the tth slot of the superframe, the CSMA/CA process of the tagged node has reached the steady state in the tth slot. Suppose the current transmission ends in the tth slot of the superframe, then the steady state probability of the last CCA performed by the tagged node in any slot ranging from the $(t - W_{M-1} + 1)$th slot (M is the maximum number of backoff stages and W_{M-1} is the maximum backoff window length of all backoff stages) to the tth slot follows the uniform distribution with a probability of P_t in each slot. Let $p_b(i, t)$ denote the probability distribution of backoff stages when the CSMA/CA process starts in the tth slot of the superframe, P_t is the reciprocal of the average backoff length.

$$P_t = \left[\sum_{i=0}^{M-1}\sum_{j=0}^{W_i-1} jp_b(i, t)/W_i\right]^{-1} = \left[\frac{1}{2}\sum_{i=0}^{M-1}(W_i - 1)p_b(i, t)\right]^{-1} \qquad (11)$$

Then after the tth slot, the probability that the tagged node performs CCA for the first time in the $(t + \mathcal{T}_b + 1)$th slot, denoted by $p_d(\mathcal{T}_b, t)$, can be determined as follows

$$p_d(\mathcal{T}_b, t) = P_t(W_{M-1} - \mathcal{T}_b)/W_{M-1}, \mathcal{T}_b = 0, 1, \ldots, W_{M-1} - 1. \qquad (12)$$

Since we have assumed that each node in the network is independent of each other, after the tth slot, the probability that the tagged node in the network firstly senses the channel in the $(t + \mathcal{T}_b)$th slot, denoted with $p_r^B(\mathcal{T}_b, t)$, is equal to the probability that all other nodes delay at least $\mathcal{T}_b$ slots.

$$p_r^B(\mathcal{T}_b, t) = p_d(\mathcal{T}_b, t)\mathbb{E}\left[\sum_{i \geq \mathcal{T}_b} p_d(i, t)\right]^{\mathcal{N}_c(t)} \tag{13}$$

The superscript $'B'$ means the variable is the result of situation discussed in this subsection and so does the superscript $'I'$ for the next subsection.

The probability that the tagged node finds the channel busy in either of the two CCA slots is the same as the probability that some other node finishes backoff process in the $(t + \mathcal{T}_b)$th slot while the tagged node completes the first backoff stage in some slot after the $(t + \mathcal{T}_b)$th slot, denoted with $p_f^B(\mathcal{T}_b, t)$, which is presented as

$$p_f^B(\mathcal{T}_b, t) = \sum_{i=\mathcal{T}_b+1}^{W_0-1} p_d(i, t)\mathbb{E}$$
$$\times \left\{\left[\sum_{i \geq \mathcal{T}_b} p_d(i, t)\right]^{\mathcal{N}_c(t)-1} - \left[\sum_{i \geq \mathcal{T}_b+1} p_d(i, t)\right]^{\mathcal{N}_c(t)-1}\right\}. \tag{14}$$

Then $p(\mathcal{T}_b, t)$ of this situation, denoted with $p^B(\mathcal{T}_b, t)$, is the summation of the two probabilities.

$$p^B(\mathcal{T}_b, t) = p_r^B(\mathcal{T}_b, t) + p_f^B(\mathcal{T}_b, t) \tag{15}$$

According to the Bayes formula, provided that some node starts a transmission from the $(t + \mathcal{T}_b + 3)$th slot, then $p_s(\mathcal{T}_b, t)$ in this situation, denoted with $p_s^B(\mathcal{T}_b, t)$, is given by

$$p_s^B(\mathcal{T}_b, t) = \frac{p_r^B(\mathcal{T}_b, t)}{p_r^B(\mathcal{T}_b, t) + p_f^B(\mathcal{T}_b, t)}. \tag{16}$$

3.4.2. Not backoff state, not the start

When a packet arrives in the tth slot of the superframe when the tagged node is idle, the tagged node begins to backoff in the $(t + 1)$th slot. Meanwhile, if the tagged node finishes the last transmission in the tth slot and there are still pending packets, the tagged node also starts a new CSMA/CA process in the $(t + 1)$th slot. For these situations, the probability that the tagged node performs CCA in $(t + \mathcal{T}_b)$th slot, $p_d'(\mathcal{T}_b, t)$ can be determined as

$$p_d'(\mathcal{T}_b, t) = 1/W_0. \tag{17}$$

It is reasonable here to make the SECOND APPROXIMATION that other nodes competing for the channel have reached steady state in the backoff process till the tth slot. Referring to Eq. (13), the probability that the tagged node first senses the channel in the $(t + \mathcal{T}_b + 1)$th slot, denoted with $p_r^I(\mathcal{T}_b, t)$, is determined by

$$p_r^I(\mathcal{T}_b, t) = p_d'(\mathcal{T}_b, t)\mathbb{E}\left[\sum_{i \geq \mathcal{T}_b} p_d(i, t)\right]^{\mathcal{N}_c(t)-1}, \tag{18}$$

where $p_d(i, t)$ is defined in Eq. (12).

Similar to Eq. (14), the failure probability of the tagged node is given by

$$p_f^I(\mathcal{T}_b, t) = \sum_{i=\mathcal{T}_b+1}^{W_0-1} p_d'(i, t)\mathbb{E}$$

$$\times \left\{\left[\sum_{i \geq \mathcal{T}_b} p_d(i, t)\right]^{\mathcal{N}_c(t)-1} - \left[\sum_{i \geq t_b+1} p_d(i, t)\right]^{\mathcal{N}_c(t)-1}\right\}. \tag{19}$$

3.4.3. Not backoff state, at the start

The behaviour of the node at the start of the superframe is different from those discussed in the above two situations. Since the duration of the inactive period is far longer than that of the active period in practical applications, packets accumulating at the beginning of the superframe are mostly those which arrive in the inactive period. Therefore, it is not reasonable to adopt the first and second approximations in this situation. We make our THIRD APPROXIMATION that if the tagged node has pending packets at the start of the superframe, all other nodes with pending packets start the CSMA/CA process in the first slot of the superframe. As a result of this approximation, the backoff length of every node is uniformly distributed in the interval $[0, W_0 - 1]$, as shown in Eq. (17). Then the probabilities that the tagged node succeeds and fails in accessing the channel after $\mathcal{T}_b$ slots are similar to Eqs. (18) and (19) with $p_d(i, t)$ substituted by $p_d'(i, t)$.

Then $p(\mathcal{T}_b, t)$ and $p_s(\mathcal{T}_b, t)$ can be determined in the same way as in Section 3.4.1.

The probabilities $p(\mathcal{T}_b, t)$ and $p_s(\mathcal{T}_b, t)$ in this situation are used separately in the queueing model while the two probabilities in Sections 3.4.1 and 3.4.2 should be merged according to the idle probability of the tth slot and the packet arrival probability. If the tagged node is idle in the tth slot and at least one packet arrives during that slot, then the case fits the situation described in Section 3.4.2. Otherwise, it belongs to the situations described in Section 3.4.1. Therefore, we can merge the probabilities in these two situations as

$$p(\mathcal{T}_b, t) = [1 - p_o(t)Q(1, 1)]p^B(\mathcal{T}_b, t) + p_o(t)Q(1, 1)p^I(\mathcal{T}_b, t), \tag{20}$$

and $p_s(\mathcal{T}_b, t)$ can be determined in the same way.

By putting $p(\mathcal{T}_b, t)$ and $p_s(\mathcal{T}_b, t)$ into equations from (3) to (8), we can calculate the steady state probabilities of the queueing model iteratively.

3.5. CSMA/CA model

To determine the virtual service time distribution of a data packet, we need to obtain the distribution of backoff stages in the CSMA/CA mechanism of IEEE 802.15.4. Fig. 4 shows the flow chat of the CSMA/CA mechanism. Five steps are involved including: (1) initializing parameters including the number of backoff stages, contention window length, and backoff exponent, and locating the backoff boundary; (2) backoff – delaying for a random number of backoff slots from $[0, 2^{BE} - 1]$; (3) requiring physical layer to perform CCA; (4) if the channel is busy, increasing the number of backoff stage and going back to step (2) on condition that $NB < macMaxNB$; if the channel is free, reducing the contention window length by one; (5) reporting success if the contention window length is zero.

The Markov-chain-based CSMA/CA model for a single node in the network under saturated condition is shown in Fig. 5. The reason why we study saturated condition is that by using the distribution of number of competing nodes from the queueing model, we can study the unsaturated condition through the behaviour of nodes in saturated networks.

Let $s(t)$ be the backoff stage counter and transmission indicator and $w(t)$ be the backoff window length counter and transmission slots counter provided that the CSMA/CA process starts in the
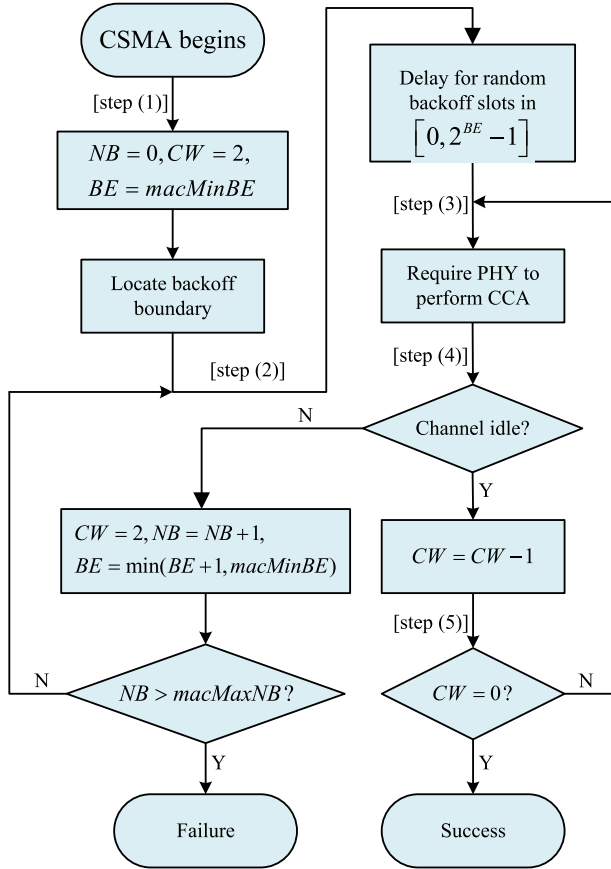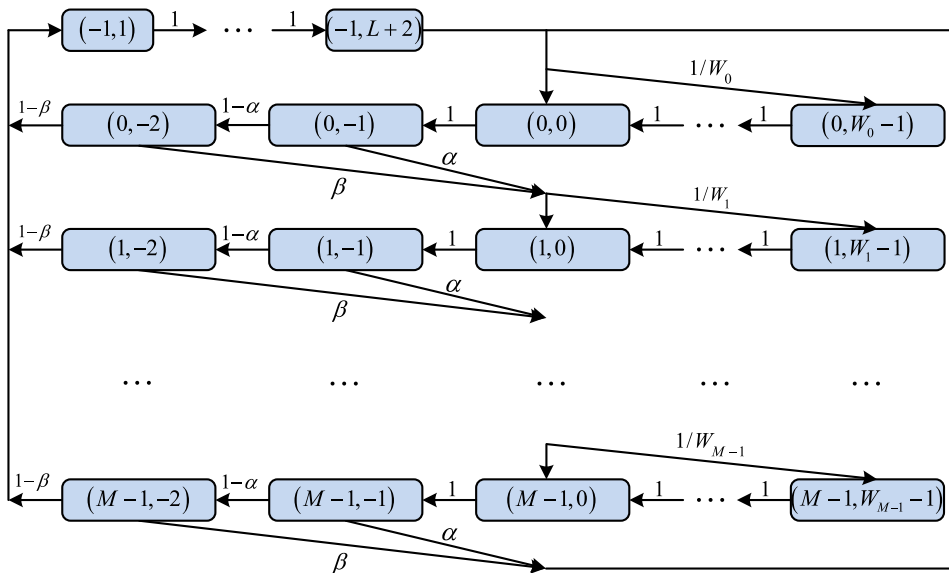
Fig. 4. CSMA/CA mechanism of IEEE 802.15.4.

Let α and β stand for the probabilities that the channel is assessed to be busy during the first CCA and during the second one provided that the first reported an idle channel, respectively. Obviously, α is the probability that there is at least one node transmitting in the network when the tagged node performs its first CCA. Derived in a similar way as [20], α is given by

$$\alpha = L\mathbb{E}\big[1 - (1 - \phi)^{\mathcal{N}_c(t)-1}\big](1 - \alpha)(1 - \beta), \qquad (21)$$

in which $\phi = \sum_{i=0}^{M-1} \varphi_{(i,0)}$. In this study, $\varphi_{(s(t), w(t))}$ is the steady state probability of state $(s(t), w(t))$ in CSMA/CA model.

Meanwhile, β is the probability that at least one node carries out the second CCA when the tagged node performs the first one.

$$\beta = \mathbb{E}\big[1 - (1 - \phi)^{\mathcal{N}_c(t)-1}\big]\big[2 - (1 - \phi)^{\mathcal{N}_c(t)}\big]^{-1} \qquad (22)$$

Notably, α and β here is time-varying rather than time-stable. From Section 3.3, the buffer of the tagged node reaches its peak at the start of the superframe and its bottom at the end. The periodic change in the buffer length influences the number of nodes competing for channel which determines α and β. Therefore, α and β depend on the location of the current slot from the start of the superframe. We take this crucial dependence which is not considered in [17] and [20] into account by recalculating these two probabilities in every CSMA/CA process.

As a result, the steady state probabilities of states in the CSMA/CA process also vary with time, which is never considered in any previous work to the best of our knowledge. This means we need to recalculate the steady state probability of each state every time the tagged node starts a new CSMA/CA process.

However, since the change of the number of competing nodes is a slow process within a superframe, we can make our FOURTH APPROXIMATION that α and β of all backoff stages in the same CSMA/CA process are the same. Therefore, although the steady state probabilities of all states in this CSMA/CA model vary with time, we can also obtain the steady state probabilities of this model in each CSMA/CA process.

Therefore, given that the tagged node is in backoff state, the probability that it currently stays in its ith backoff stage if current CSMA/CA process starts in the $(t + 1)$th slot of the superframe, denoted by $p_b(i, t)$, can be easily obtained from the steady state prob-

$(t + 1)$th slot of the superframe. Then $(s(t), w(t))$ $(s(t) = 0, \ldots, M - 1; w(t) = 0, 1, \ldots, W_{M-1} - 1)$ represents the $w(t)$th backoff state in the $s(t)$th backoff stage while $(s(t), w(t))$ $(s(t) = 0, 1, \ldots, M - 1; w(t) = -1, -2)$ stands for the $w(t)$th CCA state in the $s(t)$th backoff stage. Meanwhile, denote the $w(t)$th transmission state with $(s(t), w(t))$ $(s(t) = -1; w(t) = 1, 2, \ldots, L)$.

Fig. 5. Markov model for CSMA/CA mechanism of IEEE 802.15.4.

abilities of the CSMA/CA Markov chain $\pi_{(i,j)}$.

$$p_b(i,t) = \frac{\sum_{j=-2}^{W_i-1} \pi_{(i,j)}}{\sum_{i=0}^{M-1} \sum_{j=-2}^{W_i-1} \pi_{(i,j)}} \tag{23}$$

This mathematic model for CSMA/CA can also fit other data avoidance model with similar back-off mechanism. For instance, Virtual-Multi-Channel (VMC-) CSMA [38] can dramatically reduce delay without sacrificing the high capacity and low complexity of CSMA. The key idea of VMC-CSMA to avoid the starvation problem is to use multiple virtual channels to emulate a multi-channel system and compute a good set of feasible schedules simultaneously (without constantly switching/re-computing schedules). Q-CSMA [39] is a distributed implementation of the basic scheduling algorithm which develops a distributed randomized procedure to select a (feasible) decision schedule in the control slot by further dividing the control slot into control mini-slots. The P-persistent CSMA algorithm [40] is dedicated for control applications, which in general operate on short data packets in bursty traffic load conditions. It splits the time axis into slots and all nodes are synchronized and forced to start transmission only at the beginning of a slot. When two packets conflict, they will overlap completely rather than partially, which greatly reduces the probability of collision and provides an increase of channel efficiency.

3.6. Performance metrics

Based on the analysis of the model, we can derive the performance metrics including average number of nodes competing for channel, queue length, throughput and energy consumption in this section.

The number of nodes competing for channel in the tth slot, denoted with $N_c(t)$, follows the Binomial distribution with the idle probability of nodes. Therefore, $N_c(t)$ can be given by

$$N_c(t) = \mathbb{E}\left[i \binom{N}{i} (1-p_o(t))^i (p_o(t))^{N-i} \right], i = 0,1,2,\ldots,N. \tag{24}$$

As stated, our aim of the model is to study the time-varying characteristic of the queue length. To determine the queue length, we first suppose the queue lengths of slot t_1 and t_2 are n_1 and n_2, respectively. Then we can make reasonable approximation of the queue length in the tth slot with n_1 and n_2 as $n_q(t) = (n + \frac{t-t_1}{t_2-t_1}(n_2 - n_1))$, $(t_1 < t \leq t_2)$. Considering the impact of each state transition in the queueing model to the queue length, the queue length of the tth slot can be obtained as follows

$$L(t) = T_A \sum_{t_1 < t \leq t_2} \pi_{(n_1,t_1)} p((n_2,t_2)|(n_1,t_1)) n_q(t). \tag{25}$$

According to the preceding queueing model analysis in Section 3.3, we can see only the second category of state transitions represents packet transmissions, from which we can obtain the throughput S, i.e., average number of bits transmitted in a second. Similar to the derivation of queue length, we can also obtain the throughput by considering the impact of each state transition in the queueing model on the throughput. Denoting the average number of bits transmitted per state transition and average time consumed per state transition with S_p and T_d, respectively, we have

$$S = \frac{S_p}{T_d} = \frac{l_P \cdot \sum_{t,n,\mathcal{T}_b} \pi_{(n,t)} p(\mathcal{T}_b,t) p_s(\mathcal{T}_b,t)}{T_B \cdot \left(\sum_{t,n\mathcal{T}_b} \pi_{(n,t)} p(\mathcal{T}_b,t)\mathcal{T}_v + \sum_t \pi_{(0,t)} \right)}, \tag{26}$$

where l_P is the number of bits per packet, $t = 1,\ldots,T_A$; $n = 1,\ldots,L_m$; $\mathcal{T}_b = 1,\ldots,W_M$.

As to the energy consumption E, it can be derived using the energy consumption per state transition E_p and average number of

Parameter	Unit
Energy consumption(E)	mJ per bit
Duty cycle(D)	percent
Throughput	bits per second
Delay	slot
Queue length	/
Number of competing nodes($\mathcal{N}_c(t)$)	/
Number of nodes(N)	/
Packet arrival rate(λ)	packets per second

bits transmitted per state transition S_p.

$$E = \frac{E_p}{S_p} = \frac{E_s + E_f + E_i + E_p}{S_p}, \tag{27}$$

where E_s, E_f, E_i, and E_p are the amount of energy consumed per state transition when the node successfully accesses the channel in a state transition, fails to start a transmission in a state transition, does not contend for the channel, and comes across an inactive period, respectively.

$$E_s = T_B \sum_{t=1}^{T_A} \sum_{n=1}^{L_m} \mathbb{E}\left[\pi_{(n,t)} p_s(\mathcal{T}_b,t)(T_P P_{tx} + 2P_{rx} + \mathcal{T}_b P_{idle}) \right], \tag{28}$$

$$E_f = T_B \sum_{t=1}^{T_A} \sum_{n=1}^{L_m} \mathbb{E}\left[\pi_{(n,t)}(1 - p_s(\mathcal{T}_b,t))(P_{rx}w(t) + P_{idle}(T_P + \mathcal{T}_b + 2 - w(t))) \right], \tag{29}$$

$$E_i = T_B \sum_{t=1}^{T_A} \pi_{(0,t)} P_{idle}, \tag{30}$$

$$E_p = T_B \sum_{t=T_A-W_{M-1}+1}^{T_A} \sum_{n=0}^{L_m} \mathbb{E}\left[\pi_{(n,t)} P_{slp}|_{t+\mathcal{T}_b > T_A} \right], \tag{31}$$

in which P_{tx}, P_{rx}, P_{idle}, and P_{slp} are the power consumption for transmitting, receiving, idle, and sleep states, respectively.

4. Numerical results

The model is validated in this section by adopting a Monte Carlo simulator developed on Matlab. In the simulation scenario with a coordinator and N end nodes, all functions of the slotted CSMA/CA mechanism and the superframe structure in IEEE 802.15.4 are taken into account except for the optional contention free period. The data packets are generated by a Poisson traffic generator with the packet arrival rate λ. BO is set to be 5 and the maximum queue length is 5. According to Eq. (2), the duty cycle can be tuned by SO. The packet payload, MAC header length, and PHY header length are 107 bytes, 7 bytes and 6 bytes, respectively. The transmission rate is 250 kb/s. The initial and maximum backoff exponent are set to be 3 and 5, respectively. Each simulation data item is generated from simulation over 20,000 s. The energy parameters are set to be the same as the Chipcon CC2420 [13], in which $P_{tx} = 31.25$ mW, $P_{rx} = 35.28$ mW, $P_{idle} = 0.712$ mW, and $P_{slp} = 0.144$ uW. The TX/RX mode transition time of CC2420 is 196 us and the corresponding energy consumption is also taken into account. Other simulation parameters are set to be the default values defined in the IEEE 802.15.4 unless specified. The parameters for the simulation are in Table 2. Two types of metrics are evaluated in this section, including the essential model metrics and network performance metrics.
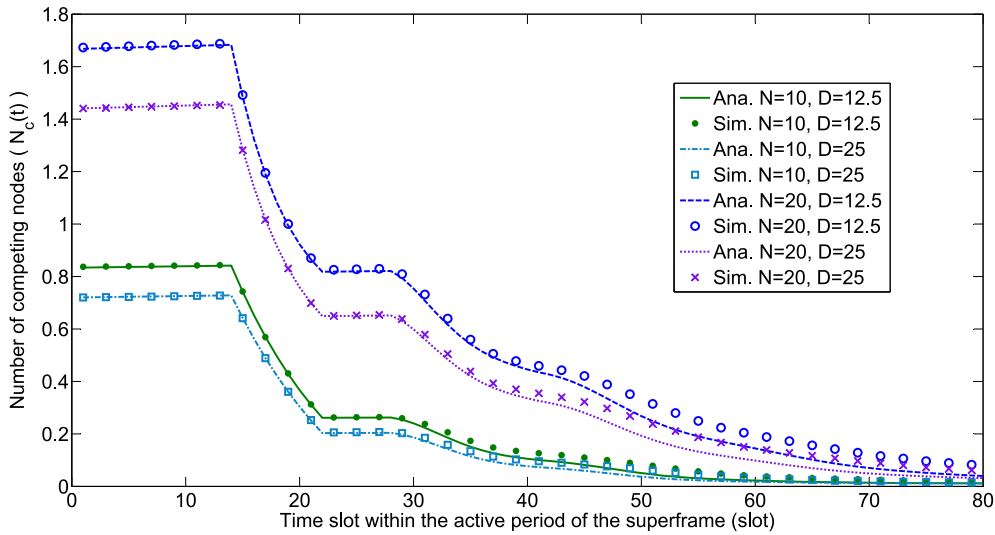
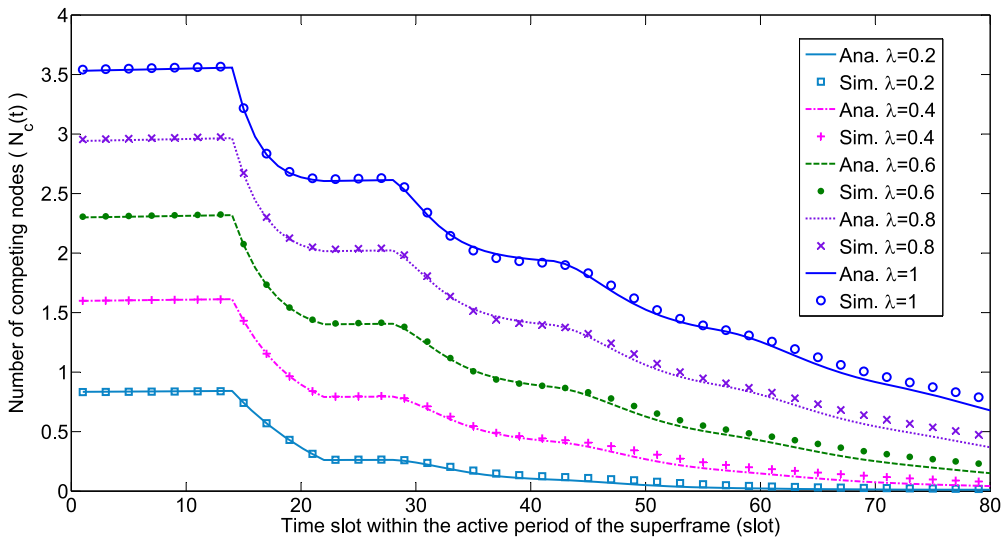**Fig. 6.** Number of competing nodes versus time within the active period ($\lambda = 0.5$).

Fig. 7. Number of competing nodes versus time within the active period ($N = 10, D = 12.5$).

4.1. Essential model metrics

Number of nodes competing for channel and queue length in each slot of the superframe are essential in the determination of the comprehensive network performance because most other network performance parameters, such as the contention intensity and packet drop rate, can be derived from these two. Therefore, the model accuracy of the number of competing nodes and queue length is most significant.

4.1.1. Number of nodes competing for channel

Figs. 6 and 7 compare the number of nodes competing for channel from both model derivations and simulations via different traffic load and number of nodes, which shows a good match. In general, the number of competing nodes becomes smaller with packet transmissions during the active portion of the superframe. Three typical features can be observed from these curves and accurately explained by our model. (1) The number of competing nodes is close to the maximum at the start of the superframe and remains nearly unchanged before it slightly goes up to its peak in the 14th slot. According to Eq. (10), the shortest virtual service time should be 14 slots (0 backoff slot, 2 CCA slots, and 12 transmission slots),

which indicates that no packets can be sent until the 15th slots. Therefore, no packet transmissions but only packet arrivals happen from the start of the inactive portion of the last superframe until the 15th slot of the current superframe, which explains the slight increase in the curve during the first 14th slots. (2) The downward trends of the curves in both figures are staged and the stages gradually fade at the end of the superframe. This can be easily explained with our virtual service time concept which has divided the superframe with virtual service time period. At the start of the superframe the virtual service time period of different nodes align with each other and thus the number of competing nodes starts decreasing sharply at the end of each virtual service time period, e.g. the 15th slot. Afterwards the staged downward trends disappear because virtual service time periods in different superframes cannot align with each other any more. (3) The number of competing nodes is smaller for a larger duty cycle. The reason lies on the fact that when the active period gets longer, each node has more time to send its packets. With the increase of number of nodes or the packet arrival rate, the number of competing nodes will apparently increase.
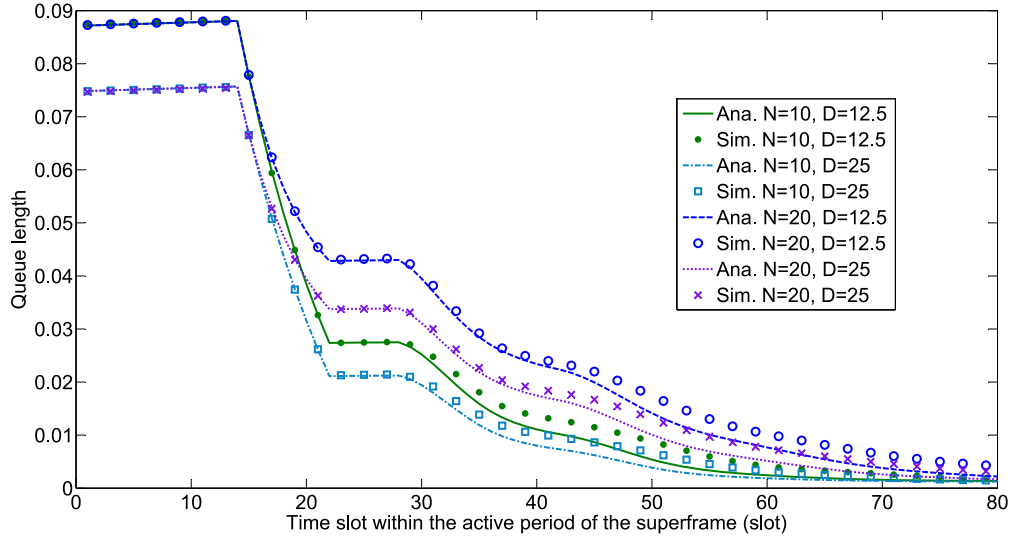
Fig. 8. Queue length versus time within the active period ($\lambda = 0.5$).
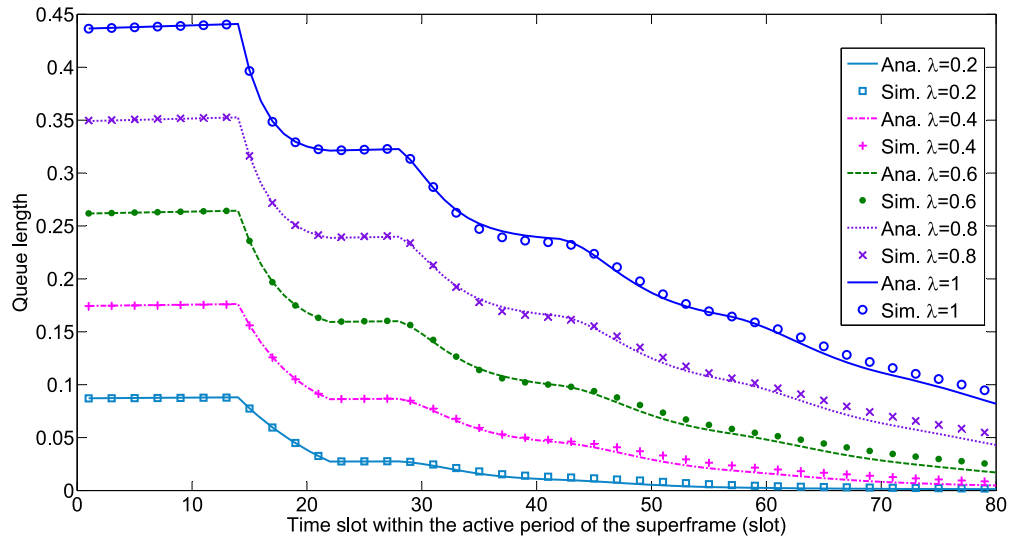

Fig. 9. Queue length versus time within the active period ($N = 10, D = 12.5$).

4.1.2. Queue length:

From Figs. 8 and 9, the queue length experiences similar trend as in Figs. 6 and 7 because the arrival and transmission of packets in the network have similar impact on the queue length of a single node and the number of nodes competing for channel in the network.

4.2. Network performance metrics

Three indispensable performance metrics, including energy consumption, packet delivery delay and throughput, are evaluated in this section.

4.2.1. Energy consumption

As shown in Figs. 10 and 11, the energy consumption goes down inversely proportionally from the start of the superframe as the growth of λ, followed by a plain till λ reaches the maximum value. From Eq. (28), the energy consumption of one bit is composed of four components including energy consumed in the transmission of the bit, CCA, idle states, and sleep states. The sleep energy only constitutes a tiny proportion due to the ultra-low sleep power consumption. Meanwhile, the transmission energy

consumption is the same for every bit. Therefore, the main factors that determine the trend of the curve are energy consumed in idle states and CCA. At the start period of the curve when λ is small and almost all packets of the node can be transmitted, the energy consumed in idle states is allocated to every bit, the number of which is directly proportional to λ. Therefore, before the start of the plain, the energy consumption is approximately inversely proportional to λ. But after the network gets saturated, the change of λ does not make a remarkable difference in the energy consumption of idle states any longer, which explains the plain in the curve.

From Fig. 10, a larger duty cycle guarantees a longer active period, so more energy is consumed in idle states when fewer packets are transmitted with a small λ. From Fig. 11, a larger number of nodes in the network lead to more intense competition for channel, thus apparently more energy consumption in CCA. With the growth of λ, the energy consumed in CCA increases slightly when duty cycle is small because competitions for channel only happen in a short period of time at the start of the superframe. Similarly, the increase in the number of nodes also lead to little more energy consumed in CCA, which explains the slightly increasing but almost plain trend in the curve. When duty cycle becomes larger
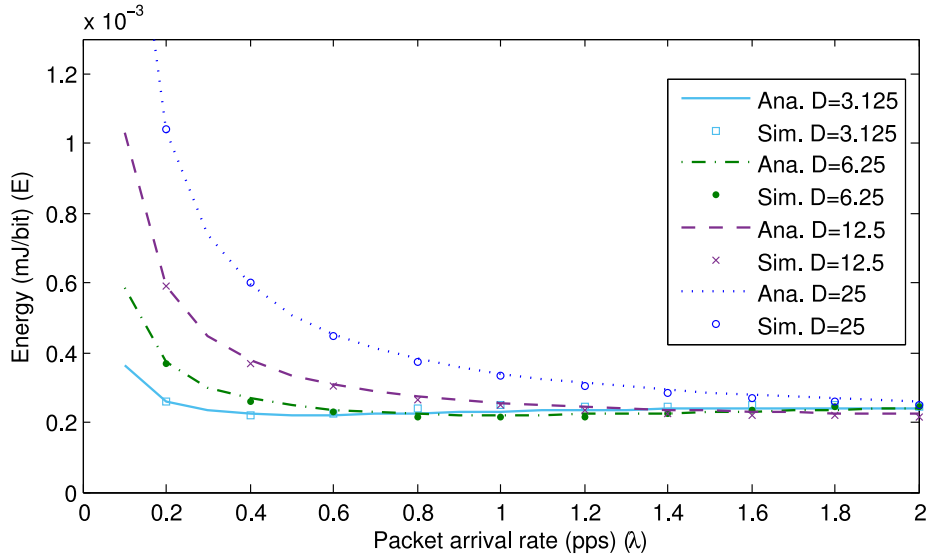
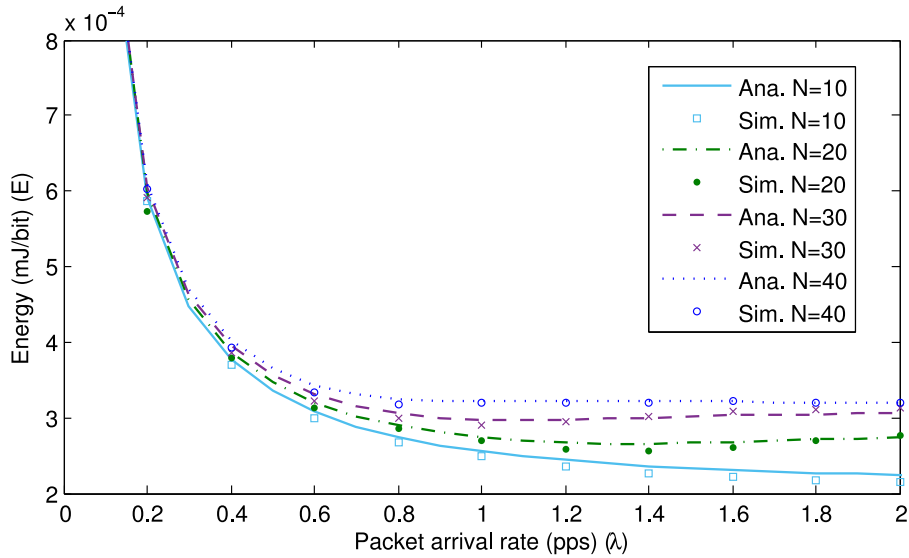**Fig. 10.** Energy consumption ($N = 10$).

Fig. 11. Energy consumption ($D = 12.5$).

or number of nodes smaller, the competitions for channel become less intense, so the curves keep decreasing slightly.

4.2.2. Packet delivery delay

Figs. 12 and 13 shows the average service delay with different duty cycles and number of nodes in the network. As we can see, when λ is small, few competitions between nodes happen in each slot so the average service delay is basically the same in different duty cycles. With the growth of λ, competitions between nodes increase accordingly, resulting in a longer average service delay.

A smaller duty cycle indicates fewer slots for transmission, leading to more intense competitions between nodes and thus larger average service delay. The network gets saturated when λ grows to a certain point, e.g. the network gets saturated when $\lambda = 1.2$ and $D = 3.125$. After this point the average service delay gets plain. It can also be observed that the delay becomes apparently larger with the increase of number of nodes in the network.

4.2.3. Throughput

Figs. 14 and 15 shows the throughput of the network. It can be observed that the throughput from model analysis matches very well with the simulations. As expected, with the growth of the packet arrival rate, the throughput of the network goes up smoothly until the network gets saturated. Once the network gets saturated with a certain packet arrival rate, the throughput levels out. For a larger duty cycle, the network capacity is also much larger because nodes in the network have more time to send their packets. With the increase of nodes, the number of pending packets grows, leading to more packet transmission failure and thus a smaller throughput.

Fig. 16 shows the impact of queue size on throughput. When λ is small, the throughput is the same for every queue with different queue size because the buffer is rarely full. But when λ is large enough to get the buffer full, some packets has to be dropped. Apparently the queue with a smaller size has to drop more packets. So with the same packet arrival rate, smaller queue size leads to smaller throughput.
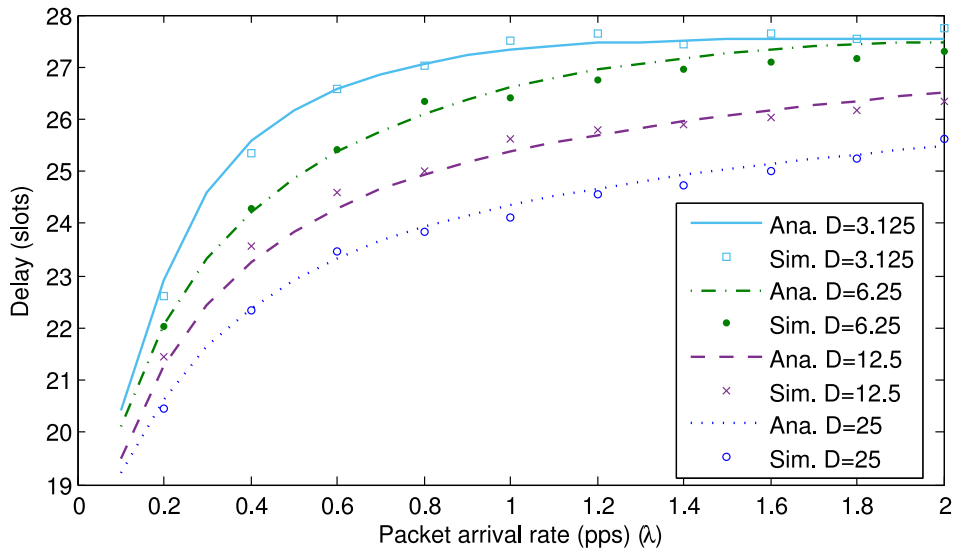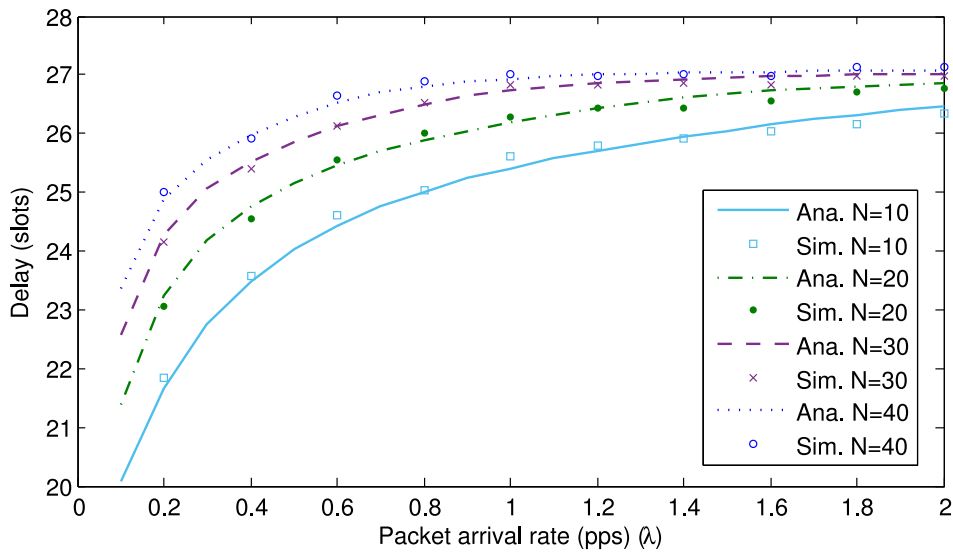
Fig. 12. Delay ($N = 10$).
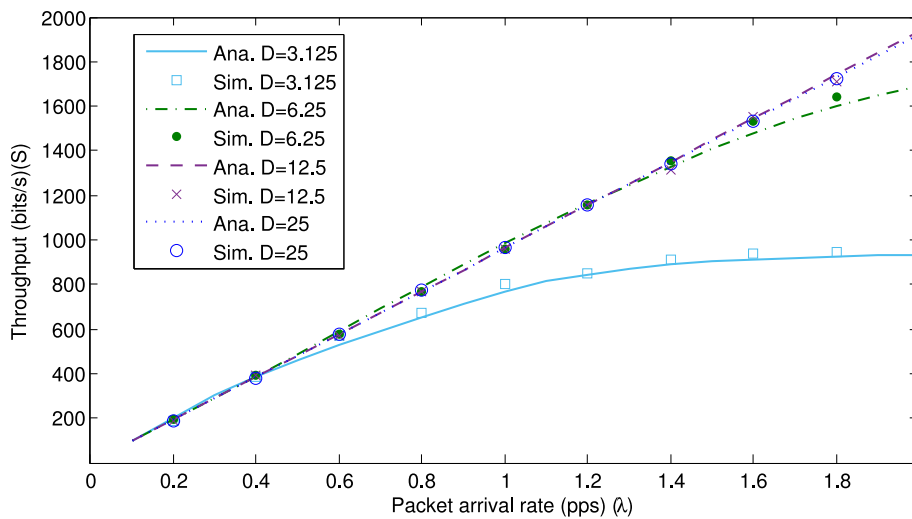

Fig. 13. Delay ($D = 12.5$).

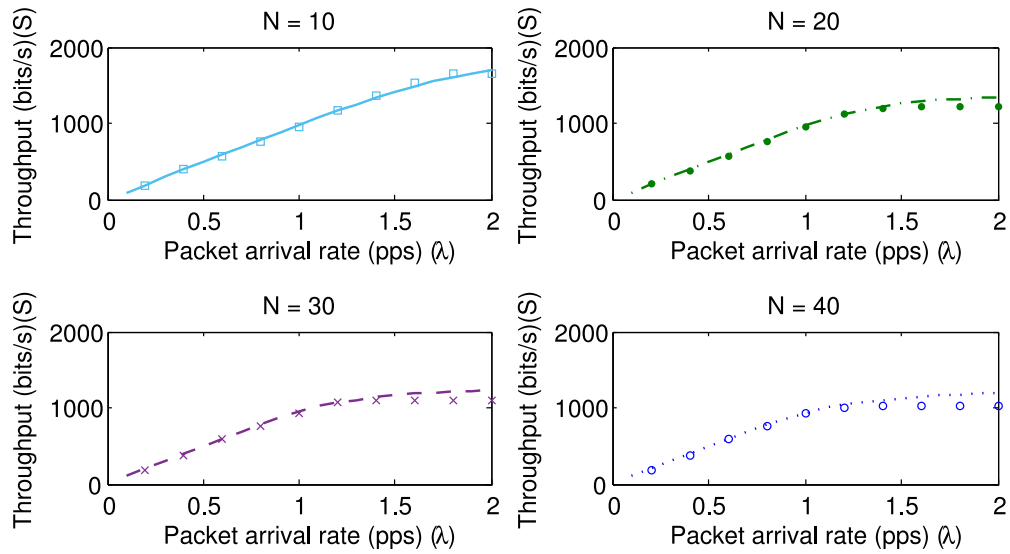

Fig. 14. Throughput ($N = 10$).
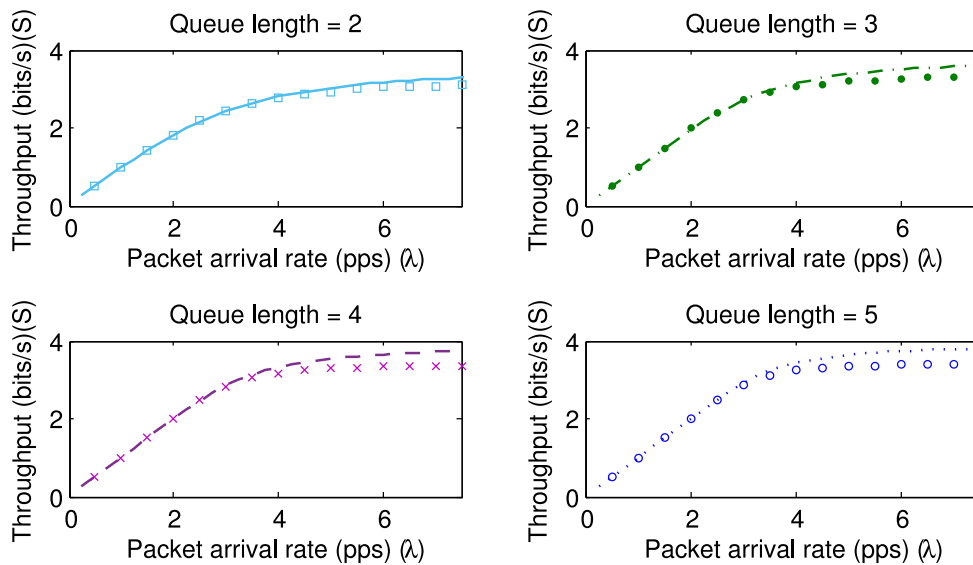
Fig. 15. Throughput ($D = 3.125$).

Fig. 16. Throughput ($N = 10, D = 12.5$).

There is a notable trend in our simulations and model derivations that the model cannot precisely predict the performance parameters with an error rate as high as 10% when the payload of the network is so large that the nodes can never empty their buffers. We can see this error rate from Figs. 15 and 16. The error comes from our THIRD APPROXIMATION because in this case when the nodes are always in CSMA/CA process, we can no longer assume that all nodes start the CSMA/CA process from the first slot of the superframe.

5. Conclusions

We have proposed a novel queueing model to analyse the time-varying characteristics of the queueing behaviour and to evaluate the performance of single-hop IEEE 802.15.4 networks. The accuracy of the model can be guaranteed because (1) the embedded discrete-time Markov chain analysis of the queueing behaviour takes into account the time-varying characteristics of the service time; and (2) we derive a virtual service time distribution instead of a service time distribution which has never been used in other studies. The analytical performance results are observed to well match the simulation results, which show that the proposed model can accurately evaluate the performance of IEEE 802.15.4.

References

[1] IEEE TG 15.4, Part 15.4: Wireless Medium Access Control (MAC) and Physical Layer (PHY) Specifications for Low-rate Wireless Personal Area Networks (WPANs), IEEE Std., New York, 2006.

[2] IEEE TG 15.4, Part 15.4: Low-rate Wireless Personal Area Networks (LR-W-PANs), IEEE Std., New York, 2011.

[3] IEEE TG 15.4, Part 15.4: Wireless Medium Access Control (MAC) and Physical Layer (PHY) Specifications for Low-rate Wireless Personal Area Networks (WPANs) Amendment 1: Add Alternate PHYs, IEEE Std., New York, 2007.

[4] IEEE TG 15.4, Part 15.4: Wireless Medium Access Control (MAC) and Physical Layer (PHY) Specifications for Low-rate Wireless Personal Area Networks (WPANs) Amendment 2: Alternative Physical Layer Extension to Support One or More of the Chinese 314C316 MHz, 430C434 MHz, and 779C787 MHz Bands, IEEE Std., New York, 2008.

[5] IEEE TG 15.4, Part 15.4: Wireless Medium Access Control (MAC) and Physical Layer (PHY) Specifications for Low-rate Wireless Personal Area Networks (WPANs) Amendment 3: Alternative Physical Layer Extension to Support the Japanese 950MHz Bands, IEEE Std., New York, 2009.

[6] M. Petrova, J. Riihijarvi, P. Mahonen, et al., Performance study of IEEE 802.15.4 using measurements and simulations, in: Proceedings of the IEEE 2016 IEEE Wireless Communications and Networking Conference (WCNC), 2006, pp. 487–492.

[7] A. Koubaa, M. Alves, E. Tovar, A comprehensive simulation study of slotted CSMA/CA for IEEE 802.15.4 wireless sensor networks, in: Proceedings of the IEEE International Workshop Factory Communication System, 2006, pp. 183–192.

[8] C. Buratti, R. Verdone, On the number of cluster heads minimizing the error rate for a wireless sensor network using a hierarchical topology over IEEE 802.15.4, in: Proceedings of the IEEE 17th International Symposium Personal, Indoor and Mobile Radio Communications (PIMRC), 2006 1-6.

[9] J.S. Lee, Performance evaluation of IEEE 802.15.4 for low-rate wireless personal area networks, IEEE Trans. Consum. Electron. 52 (3) (2006) 742–749.

[10] A. Kouba, A. Cunha, M. Alves, A Time Division Beacon Scheduling Mechanism for IEEE 802.15.4/Zigbee Cluster-tree Wireless Sensor Networks, in: Proc. 20th Euromicro Conf. Real-Time Syst. (ETFA), 2007, pp. 125–135.

[11] J. Mišić, S. Shafi, V.B. Mišić, The impact of MAC parameters on the performance of 802.15.4 PAN, Ad Hoc Netw. 3 (5) (2005) 509–528.

[12] J. Mišić, S. Shafi, V.B. Mišić, Maintaining reliability through activity management in an 802.15.4 sensor cluster, IEEE Trans. Veh. Technol. 55 (3) (2006) 779–788.

[13] I. Ramachandran, A.K. Das, S. Roy, Analysis of the contention access period of IEEE 802.15.4 MAC, ACM Trans. Sens. Netw. 3 (1) (2007) 1706–1718.

[14] T.R. Park, T.H. Kim, J.Y. Choi, et al., Throughput and energy consumption analysis of IEEE 802.15.4 slotted CSMA/CA, IEEE Electron. Lett. 41 (18) (2005) 1017–1019.

[15] A. Koubaa, M. Alves, E. Tovar, gts allocation analysis in IEEE 802.15.4 for real–time wireless sensor networks, in: Proceedings 20th IEEE International Parallel and Distributed Processing Symposium, Rhodes Island, 8, 2006.

[16] S.e. Yoo, et al., Guaranteeing real-time services for industrial wireless sensor networks with IEEE 802.15.4, IEEE Trans. Ind. Electron. 57 (11) (2010) 3868–3876.

[17] G. Bianchi, Performance analysis of the IEEE 802.11 distributed coordination function, IEEE J. Select. Areas Commun. 18 (3) (2000) 535–547.

[18] Y. Zhang, P. Xu, Z. Zhang, et al., Comments on throughput analysis of IEEE 802.15.4 slotted CSMA/CA considering timeout period, IEEE Electron. Lett. 42 (19) (2006) 1127–1128.

[19] J. He, Z. Tang, H.H. Chen, et al., An accurate markov model for slotted CSMA/CA algorithm in IEEE 802.15.4 networks, IEEE Commun. Lett. 12 (6) (2008) 420–422.

[20] S. Pollin, M. Ergen, S.C. Ergen, et al., Performance analysis of slotted carrier sense IEEE 802.15.4 medium access layer, IEEE Trans. Wirel. Commun. 7 (9) (2008) 3359–3371.

[21] J. He, Z. Tang, H.H. Chen, et al., An accurate and scalable analytical model for IEEE 802.15.4 slotted CSMA/CA networks, IEEE Trans. Wirel. Commun. 8 (1) (2009) 440–448.

[22] C. Buratti, Performance analysis of IEEE 802.15.4 beacon-enabled mode, IEEE Trans. Veh. Technol. PP (99) (2010) 1.

[23] Z. Xiao, C. He, L. Jiang, Slot-based model for IEEE 802.15.4 MAC with sleep mechanism, IEEE Commun. Lett. 14 (2) (2010) 154–156.

[24] P. Park, P. Marco, C. Fischione, K. Johansson, Modeling and optimization of the IEEE 802.15.4 protocol for reliable and timely communications, IEEE Trans. Parallel and Distrib. Syst. 24 (3) (2013) 550–564.

[25] N. Karowski, A. Viana, A. Wolisz, Optimized asynchronous multichannel discovery of IEEE 802.15.4-based wireless personal area networks, IEEE Trans. Mobile Comput. 12 (10) (2013) 1972–1985.

[26] J. Zhu, Z. Tao, C. Lv, Performance improvement for IEEE 802.15.4 CSMA/CA scheme in large-scale wireless multi-hop sensor networks, IET Wirel. Sens. Syst. 3 (2) (2013) 93–103.

[27] I. Al-Anbagi, M. Erol-Kantarci, H. Mouftah, A reliable IEEE 802.15.4 model for cyber physical power grid monitoring systems, IEEE Trans. Emerg. Topics Comput. 1 (2) (2013) 258–272.

[28] F. Martelli, C. Buratti, R. Verdone, Modeling query-based wireless CSMA networks through stochastic geometry, IEEE Trans. Veh. Technol. 63 (6) (2014) 2876–2885.

[29] B. Bandyopadhyay, S.J. Ahmed, D. Das, A. Chatterjee, AS 802.15.4: a modified IEEE 802.15.4 standard for more reliable communication and utilization of inactive period using optimized sleep period, in: Proceedings of the 2014 Annual IEEE India Conference (INDICON), Pune, 2014, pp. 1–6.

[30] D.H. Lee, H.T. Roh, B.G. Kim, J.W. Lee, Performance Analysis of the IEEE 802.15.4MAC Protocol, in: Proceedings of the 2013 International Conference on ICT Convergence (ICTC), Jeju, 2013, pp. 398–401.

[31] D. Striccoli, G. Boggia, L.A. Grieco, A markov model for characterizing IEEE 802.15.4 MAC layer in noisy environments, IEEE Trans. Ind. Electron. 62 (8) (2015) 5133–5142.

[32] K. Govindan, A.P. Azad, K. Bynam, S. Patil, T. Kim, Modeling and analysis of non beacon mode for low-rate WPAN, in: Proceedings of the 2015 12th Annual IEEE Consumer Communications and Networking Conference (CCNC), Las Vegas, NV, 2015, pp. 549–555.

[33] J. Mišić, V.B. Mišić, Performance of a beacon enabled IEEE 802.15.4 cluster with downlink and uplink traffic, IEEE Trans. Parallel Distrib. Syst. 17 (4) (2006) 361–376.

[34] Y.K. Huang, A.C. Pang, H.N. Hung, A comprehensive analysis of low-power operation for beacon-enabled IEEE 802.15.4 wireless networks, IEEE Trans. Wirel. Commun. 8 (11) (2009) 5601–5611.

[35] Z. Xiao, C. He, L. Jiang, An analytical model for IEEE 802.15.4 with sleep mode based on time-varying queue, in: Proceedings of the International Conference Communication (ICC'11), 2011, pp. 1–5.

[36] S. Singh, C.S. Raghavendra, PAMAS: Power aware multi-access protocol with signaling for ad hoc networks, ACM Comput. Comm. Rev. 28 (3) (1998) 5–26.

[37] C. Li, H. Li, R. Kohno, Performance evaluation of IEEE 802.15.4 for wireless body area network (WBAN), in: Proceedings of the International Conference Communication (ICC'06), 2009, pp. 1–5.

[38] P.K. Huang, X. Lin, Improving the delay performance of CSMA algorithms: a virtual multi-channel approach, in: Proceedings of the IEEE INFOCOM, 2013, pp. 2598–2606.

[39] J. Ni, B. Tan, R. Srikant, Q-CSMA: Queue-length-based CSMA/CA algorithms for achieving maximum throughput and low delay in wireless networks, IEEE/ACM Trans. Netw. 20 (3) (2012) 825–836.

[40] M. Miskowicz, M. Sapor, M. Zych, W. Latawiec, Performance analysis of predictive p-persistent CSMA protocol for control networks, in: Proceedings of the IEEE International Workshop on Factory Communication Systems, 2002, pp. 249–256.

Zhuoling Xiao is an Associate Professor at the University of Electronic Science and Technology of China. He obtained his Ph.D at University of Oxford, became a postdoctoral researcher at University of Oxford. His interests lie in localization protocols for networked sensor nodes and machine learning techniques for sensor networks and localization. Zhuoling has several international patent applications and over 30 papers published in leading journals and conferences including several best paper awards from leading conferences including IPSN and EWSN.

Jie Zhou is currently a M.Sc candidate in the Department of Internet of Things at University of Electronic Science and Technology of China. His research interests focus on sensor networks, including localization, and machine learning techniques for sensor networks and localization.

Junjie Yan is currently a Bachelor candidate in School of Communication Engineering at University of Electronic Science and Technology of China. His research interests focus on the application of machine learning techniques in sensor networks and localization.

Chen He (S'93–M'96) received the B.E. and M.E. degrees in electronic engineering from Southeast University of China in 1982 and 1985, respectively, and the Ph.D. degree in electronics system from Tokushima University of Japan in 1994. He was with the Department of Electronic Engineering, Southeast University of China, from 1985 to 1990. He joined the Department of Electronic Engineering, Shanghai Jiao Tong University of China, Shanghai, China, in 1996. He visited the Tokushima University of Japan as a foreign researcher from October 1990 to September 1991, and visited the Communication Research Laboratory of Japan from December 1999 to December 2000 as a research fellow. He has published more than 200 journal papers and over 80 conference papers. Currently, he is a Professor and Vice Director of Advanced Communication Institute, Shanghai Jiao Tong University. His current research interests are 4G wireless communication systems, wireless sensor network, and signal processing. Dr. He received the best paper award in Globecom 2007.

Lingge Jiang (M'03) received the B.E. degree in radio engineering from the Southeast University of China in 1982, and the M.E. and Ph.D. degrees in electrical engineering from Tokushima University of Japan, in 1993 and 1996, respectively. She joined the Department of Electronic Engineering, Shanghai Jiao Tong University, Shanghai, China, in 1996. Currently, she is a professor with Shanghai Jiao Tong University. Her current research interests include wireless communication systems, wireless sensor networks, and intelligent information processing.

Niki Trigoni is a Professor at the Oxford University Department of Computer Science and a fellow of Kellogg College. She obtained her DPhil at the University of Cambridge (2001), became a postdoctoral researcher at Cornell University (2002–2004), and a Lecturer at Birkbeck College (2004–2007). At Oxford, she is currently Director of the EPSRC Centre for Doctoral Training on Autonomous Intelligent Machines and Systems, a program that combines machine learning, robotics, sensor systems and verification/control. She also leads the Cyber Physical Systems Group, which is focusing on intelligent and autonomous sensor systems with applications in positioning, healthcare, environmental monitoring and smart cities. The group's research ranges from novel sensor modalities and low level signal processing to high level inference and learning.